

p66Shc deficiency in the E μ -TCL1 mouse model of chronic lymphocytic leukemia enhances leukemogenesis by altering the chemokine receptor landscape

Laura Patrussi,¹ Nagaja Capitani,^{1,2} Cristina Ulivieri,¹ Noemi Manganaro,¹ Massimo Granai,³ Francesca Cattaneo,¹ Anna Kabanova,¹ Lucia Mundo,³ Stefania Gobessi,⁴ Federica Frezzato,^{5,6} Andrea Visentin,^{5,6} Francesca Finetti,¹ Pier Giuseppe Pelicci,⁷ Mario M. D'Ellos,² Livio Trentin,^{5,6} Gianpietro Semenzato,^{5,6} Lorenzo Leoncini,³ Dimitar G. Efremov⁴ and Cosima T. Baldari¹

¹Department of Life Sciences, University of Siena, Siena; ²Department of Clinical and Experimental Medicine, University of Florence, Florence; ³Department of Human Biotechnologies, University of Siena, Siena; ⁴International Center for Genetic Engineering and Biotechnology, Trieste; ⁵Venetian Institute of Molecular Medicine, Padua; ⁶Department of Medicine, Hematology and Clinical Immunology Branch, Padua University School of Medicine, Padua and ⁷European Institute of Oncology, Milan, Italy

©2019 Ferrata Storti Foundation. This is an open-access paper. doi:10.3324/haematol.2018.209981

Received: October 22, 2018.

Accepted: February 22, 2019.

Pre-published: February 28, 2019.

Correspondence: *COSIMA T. BALDARI* - baldari@unisi.it

LAURA PATRUSSI - patrussi2@unisi.it

Supplemental Methods

Screening strategy of mice

DNA and RNA were extracted from ≥ 20 μ l PB of C57BL/6J, C57/p66^{-/-}, E μ -TCL1 and E μ -TCL1/p66Shc^{-/-} mice using PureLink Genomic DNA minikit (Thermo Fisher Scientific, Waltham, USA) and NucleoSpin RNA Blood (Macherey-Nagel, Düren, Germany). PCR settings (primers listed in Table S3): 3 min 95°C, 40 cycles 30 sec 95°C, 30 sec 63°C, 30 sec 72°C, 7 min 72°C. Mice were monitored for leukemia development by monthly white blood cell (WBC) counts (Trypan Blue exclusion) and flow cytometric quantification of % CD5⁺IgM⁺CD19⁺ cells.

Screening of Trp53 mRNA by PCR

Total RNA was extracted and retrotranscribed from CD19⁺CD5⁺ cells purified by immunomagnetic sorting from E μ -TCL1 (n=7) and E μ -TCL1/p66Shc^{-/-} (n=11) mice using mouse B1a Cell Isolation Kit (Miltenyi Biotech), as reported.¹ Three primer pairs generating 3 partially overlapping fragments to cover the entire cDNA sequence were designed on the Trp53 transcript variant 1 (NM_011640.3) (primers listed in Table S3). PCR settings: 5 min 95°C; 35 cycles 1 min 94°C, 1 min and 30 sec 60°C; 7 min 72°C. PCR fragments were purified (Macherey-Nagel) and subjected to DNA sequencing.

Cell lines, patients and healthy donors

Diagnosis of CLL was made according to international workshop of CLL (iwCLL) 2008 criteria.² Diameters of superficial lymph nodes (LNs) (cervical, clavicular, axillary, inguinal and crural) as well as hepatic and spleen margins below costal ribs were determined by physical examination and ultrasound in non-progressive patients or by computer

tomography scan in progressive patients. Mutational *IGHV* status was assessed as reported.³

PB was collected from 5 CLL patients treated first line with chemoimmunotherapy. Patients from #1 to #3 received FCR (fludarabine 25 mg/ml plus cyclophosphamide 250 mg/ml administered on day 1-3 of cycles 1-6 and rituximab 375 mg/ml on day 1 of cycle 1 and 500 mg/ml on day 1 of cycles 2-6). Patients #4 and 5# received BR (bendamustine 90 mg/ml administered on day 1-2 of cycles 1-6 and rituximab 375 mg/ml on day 1 of cycle 1 and 500 mg/ml on day 1 of cycles 2-6). These treatments were started at disease progression according to iwCLL criteria.² FCR and BR are two commonly used first-line therapy for CLL.² At disease relapse all patients were managed with ibrutinib 420 mg once a day.⁴ From each patient, PB samples were collected within 1 month before starting chemoimmunotherapy, 2 months after the last cycle of chemoimmunotherapy, the starting day of ibrutinib treatment and during follow-up. Patients were grouped in “responding”, i.e. those achieving at least a partial response to ibrutinib, and in “failing”, i.e. those experiencing disease progression during treatment with ibrutinib.^{2,4}

CLL cells were cotransfected with 1 μ g GFP reporter/sample and 5 μ g pcDNA3 or p66Shc-encoding pcDNA3 using Human B-cell Nucleofector Kit (Amaxa Biosystems, Cologne, Germany). Transfection efficiency was ~40%, as assessed by flow cytometry of GFP⁺ cells, and cell viability 48 h post-transfection was 40-60%.

Purification of murine B cell populations

B1a, B1b and B2 cells were purified from age-matched 9-12-month-old C57BL/6J or E μ -TCL1 mice by immunomagnetic activated cell-sorting (MACS, Miltenyi Biotech). Splenic B cells were purified from C57BL/6J or E μ -TCL1 mice as reported.⁵

In vitro leukemic cell treatment

The concentration of fludarabine phosphate used in this work was determined by analyzing the % of Annexin-V⁺/PI⁻ C57BL/6J splenocytes incubated for 16 h with either DMSO or 3.5, 10 or 35 μ M fludarabine phosphate (19.7 \pm 0.5%, 27.6 \pm 4.2%, 63 \pm 3.1% and 65 \pm 7.2, respectively). 35 μ M fludarabine phosphate, which elicited the highest apoptotic response in the preliminary tests, was used for all subsequent experiments.

Histopathology and Immunohistochemistry

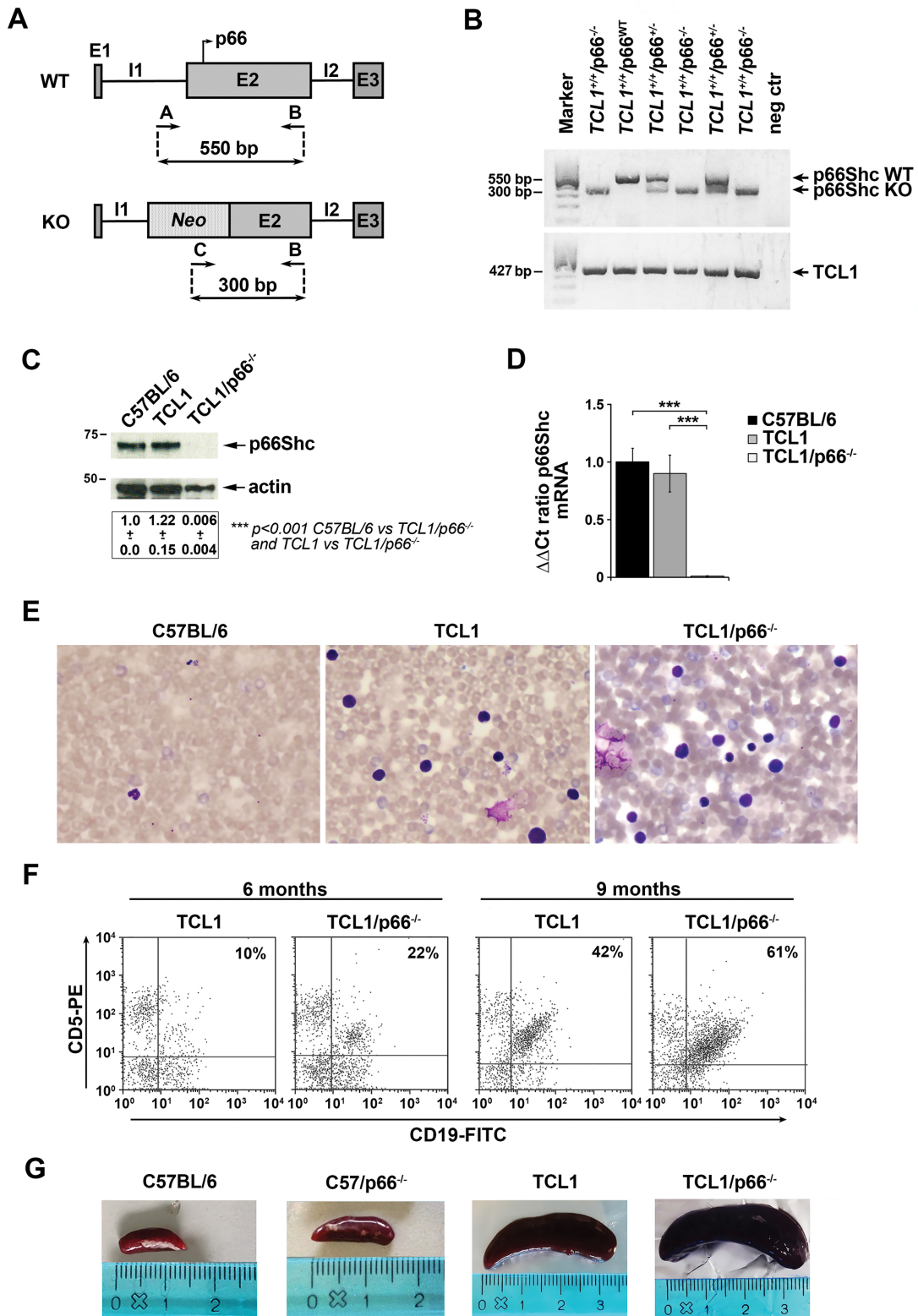
PB and PW were collected, stained 5 min in May-Grünwald and then 30 min in Giemsa. Organ homogenates were passed through 70- μ m cell strainers and the percentage of CD5⁺CD19⁺ cells was assessed by flow cytometry. H&E staining and CD45R immunohistochemical analysis of the organs were performed as described.⁶ CD45R immunohistochemical analysis of the organs was carried out on Bond III automated immunostainer (Leica Microsystem, Bannockburn, IL, USA) and diaminobenzidine (DAB, Leica Microsystem, Bannockburn, IL, USA) was used as chromogen.

Study approval

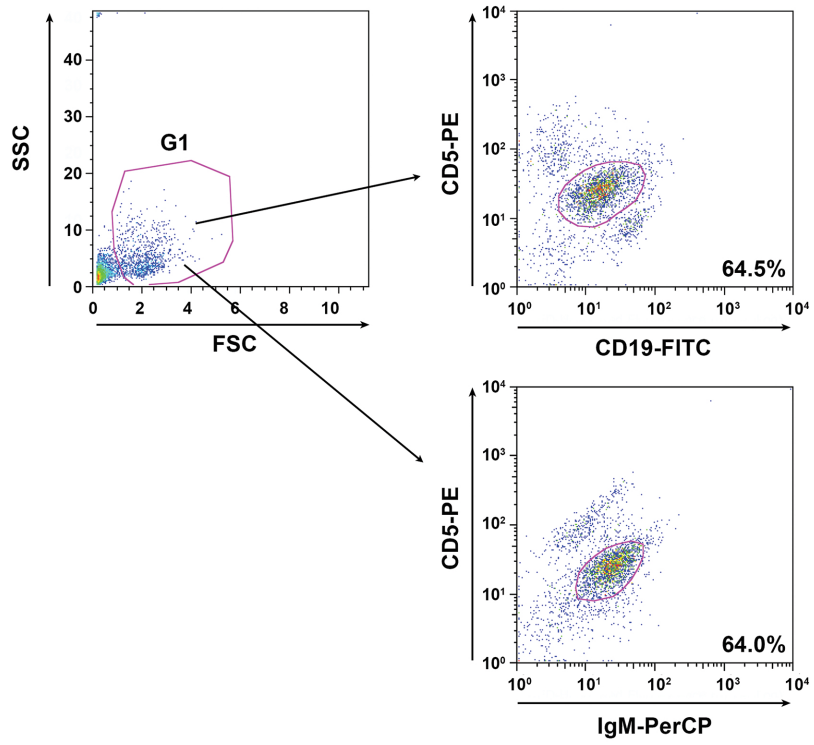
Prior written informed consent was received from CLL patients and healthy donors according to the Helsinki Declaration. Experiments were approved by the local Ethics Committee. Animal procedures were carried out in agreement with the Guiding Principles for Research Involving Animals Beings and approved by the local ethical committee and the Italian Health Ministry.

Supplemental references

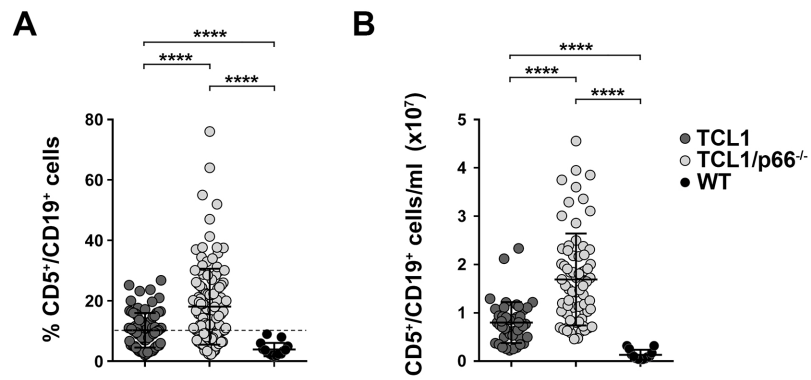
1. Capitani N, Patrussi L, Trentin L, et al. S1P1 expression is controlled by the pro-oxidant activity of p66Shc and is impaired in B-CLL patients with unfavorable prognosis. *Blood* 2012;120(22):4391–4399.
2. Eichhorst B, Fink A-M, Bahlo J, et al. First-line chemoimmunotherapy with bendamustine and rituximab versus fludarabine, cyclophosphamide, and rituximab in patients with advanced chronic lymphocytic leukaemia (CLL10): an international, open-label, randomised, phase 3, non-inferiority trial. *Lancet Oncol* 2016;17(7):928–942.
3. Visentin A, Facco M, Frezzato F, et al. Integrated CLL Scoring System, a New and Simple Index to Predict Time to Treatment and Overall Survival in Patients with Chronic Lymphocytic Leukemia. *Clin Lymphoma, Myeloma Leuk* 2015;15(10):612–620e5.
4. Brown JR, Hillmen P, O'Brien S, et al. Extended follow-up and impact of high-risk prognostic factors from the phase 3 RESONATE study in patients with previously treated CLL/SLL. *Leukemia* 2018;32(1):83–91.
5. Patrussi L, Capitani N, Cattaneo F, et al. p66Shc deficiency enhances CXCR4 and CCR7 recycling in CLL B cells by facilitating their dephosphorylation-dependent release from β -arrestin at early endosomes. *Oncogene* 2018;37(11):1534–1550.
6. Yasuda M, Ogura T, Goto T, et al. Incidence of spontaneous lymphomas in non-experimental NOD/Shi-scid, IL-2R γ null (NOG) mice. *Exp Anim* 2017;66(4):425–435.



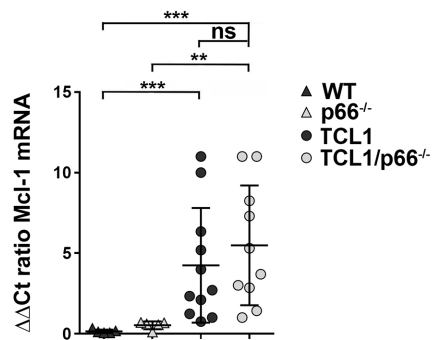
Supplemental Figure S1



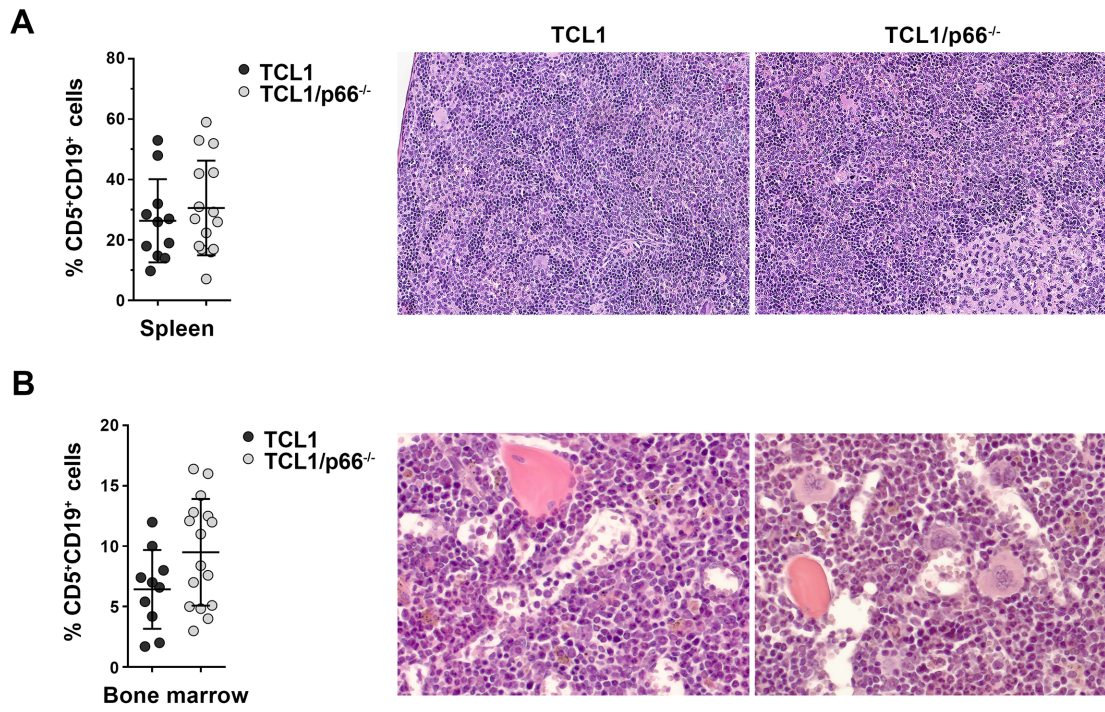
Supplemental Figure S2



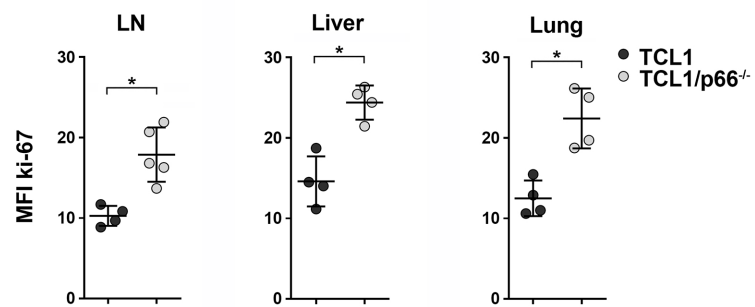
Supplemental Figure S3



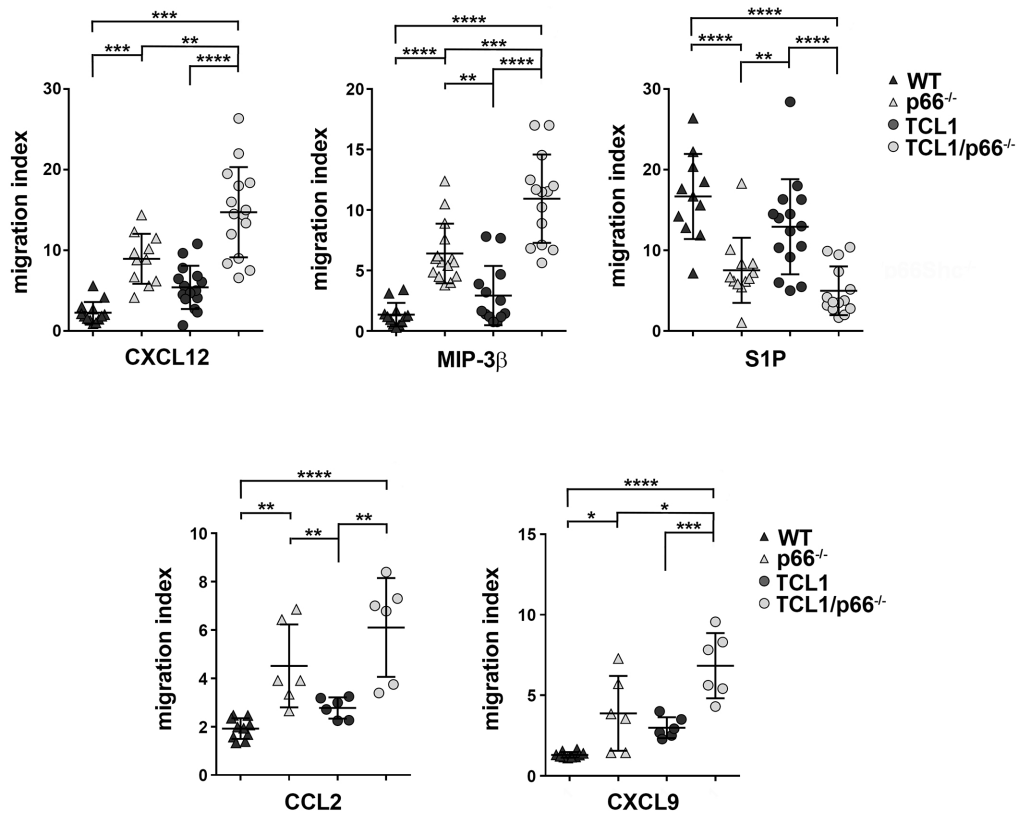
Supplemental Figure S4



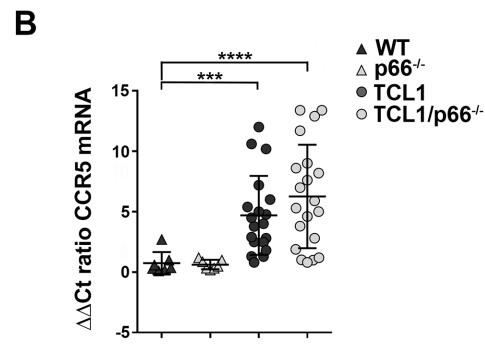
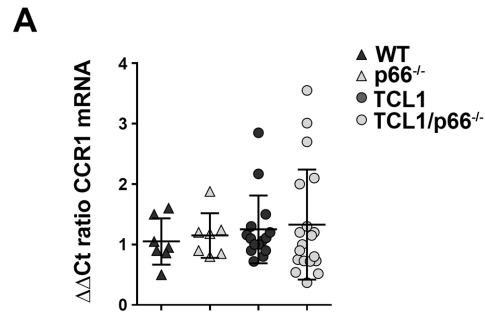
Supplemental Figure S5



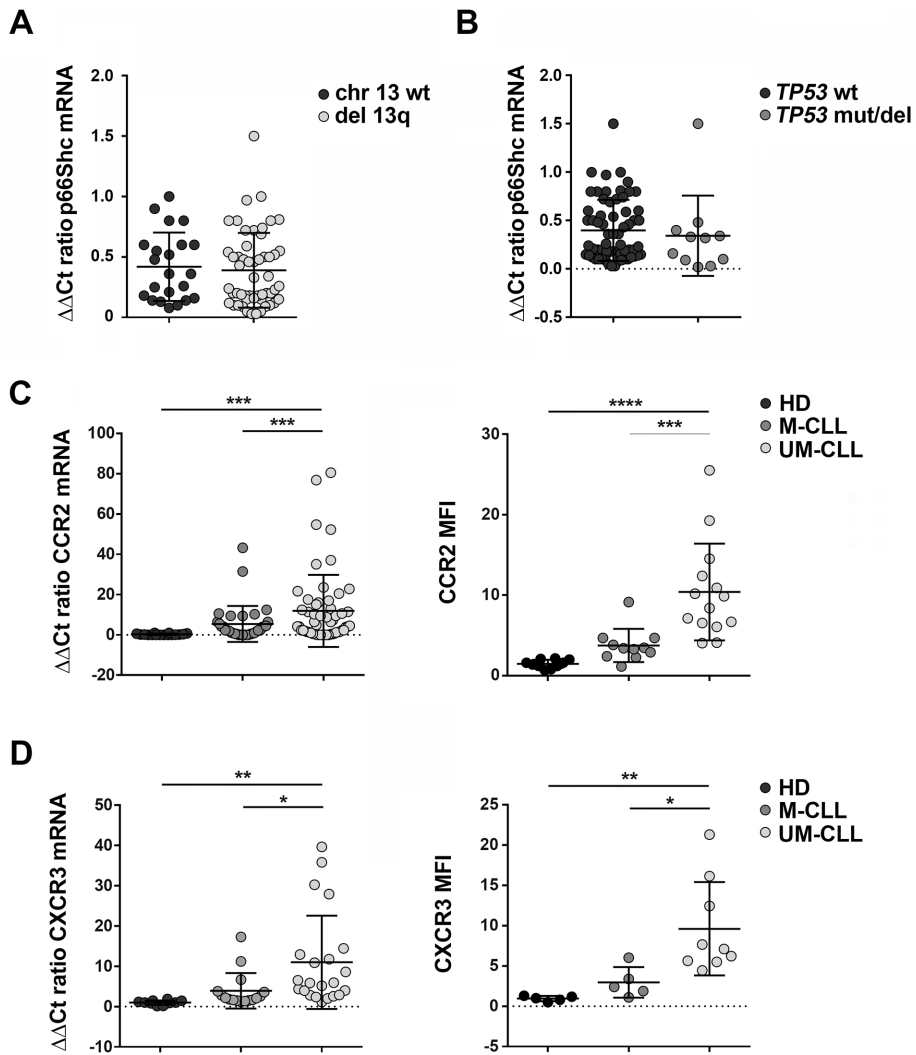
Supplemental Figure S6



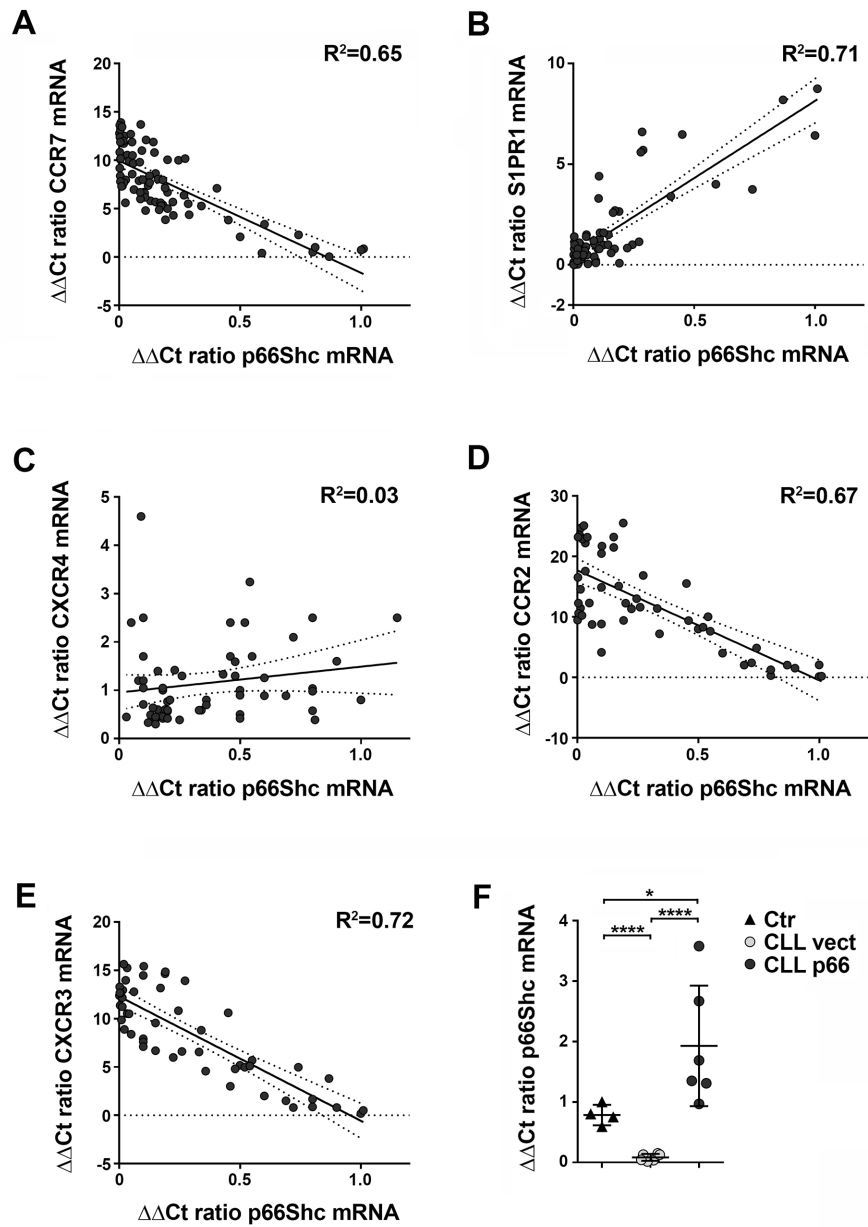
Supplemental Figure S7



Supplemental Figure S8

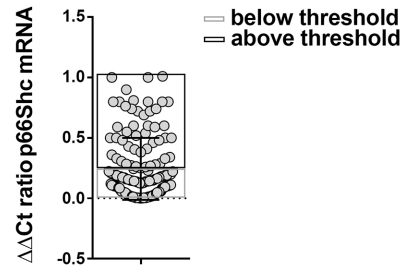


Supplemental Figure S9

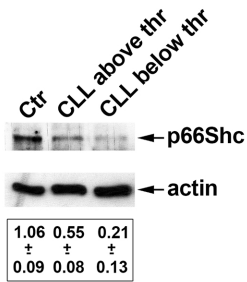


Supplemental Figure S10

A



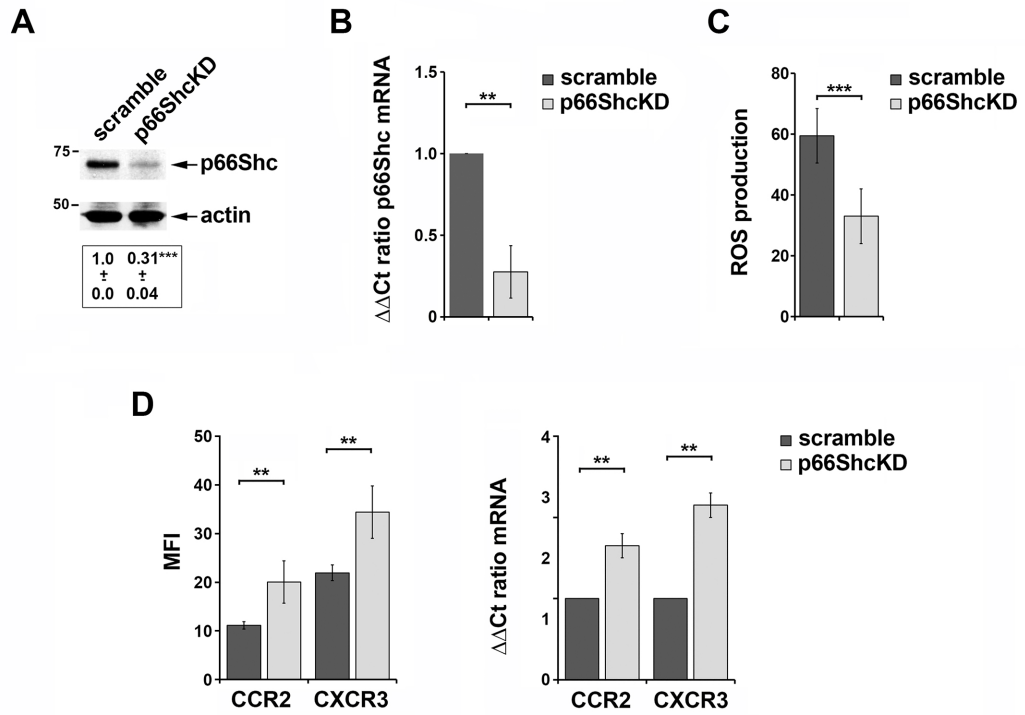
B



** $p < 0.01$ Ctr vs CLL above thr/below thr

*** $p < 0.001$ CLL above thr vs below thr

Supplemental Figure S11



Supplemental Figure S12

Legends to Supplementary figures

Figure S1. A. Schematic representation of the wild-type (WT) and knock-out (KO) alleles of *p66Shc*. Primers A, B and C used in the screening strategy, as well as the length of the relative amplicons, are indicated. **B.** PCR analysis of wild-type (WT) and knock-out (KO) *p66Shc* alleles in genomic DNA from peripheral blood of selected mice undergoing screening. PCR analysis of TCL1 was performed on cDNA obtained by retro-transcription of mRNA extracted from the same blood samples. **C, D.** Immunoblot analysis of Shc expression (**C**) and quantitative RT-PCR analysis of p66Shc mRNA (**D**) in B cells purified from spleens of TCL1 (n=3), TCL1/p66Shc^{-/-} (n=3) or C57BL/6 wild-type mice (n=3) collected at 2 months of age. A control anti-actin blot of the stripped filter is shown below. The migration of molecular mass markers is indicated (**C**). The relative gene transcript abundance was determined on triplicate samples using the ddCt method (**D**). **E.** Smears of blood obtained from wild-type, E μ -TCL1 and E μ -TCL1/p66^{-/-} mice with overt leukemia. Slides were stained with Wright-Giemsa. Original magnification, 40x. **F.** Flow cytometric analysis of the percentages of CD5⁺CD19⁺ cells in peripheral blood samples from either E μ -TCL1 or E μ -TCL1/p66Shc^{-/-} mice collected at the indicated months. The figure shows representative flow cytometric plots. **G.** Representative photographs of spleens harvested from wild-type and p66Shc^{-/-} mice, and from E μ -TCL1 and E μ -TCL1/p66Shc^{-/-} mice with overt leukemia. Mean \pm SD. Anova one-way test, Multiple Comparison. p \leq 0.0001, ****.

Figure S2. Gating strategy of a representative E μ -TCL1 mouse peripheral blood sample, stained with CD5-PE, IgM-PerCP and CD19-FITC antibodies. Panels showing stained cells (right) represent cells included in gate G1 (left).

Figure S3. Flow cytometric analysis of the percentages of CD5⁺CD19⁺ cells (**A**) and numbers of WBC / ml (**B**) in peripheral blood samples from E μ -TCL1 (n=73), E μ -TCL1/p66Shc^{-/-} (n=81) or wild-type mice (n=10) collected at 6 months of age. Mean \pm SD. Anova one-way test, Multiple Comparison. p \leq 0.001, ***.

Figure S4. Quantitative RT-PCR analysis of Mcl-1 mRNA in leukemic cells purified from either wild-type (n=7) or p66Shc^{-/-} (n=7) mice and from E μ -TCL1 (n=11) or E μ -TCL1/p66Shc^{-/-} (n=10) mice with overt leukemia. The relative gene transcript abundance was determined on triplicate samples using the ddCt method. Mean \pm SD. Mann Whitney Rank Sum test. p \leq 0.001, ***; p \leq 0.01, **.

Figure S5. Flow cytometric analysis of the percentages of CD5⁺CD19⁺ cells in spleen (**A**) and bone marrow (**B**) of either E μ -TCL1 or E μ -TCL1/p66Shc^{-/-} mice with overt leukemia. Mean \pm SD. Error bars, SD p>0.05, non-significant, Mann Whitney Rank Sum test. H&E staining of spleen (**A**) and bone marrow (**B**) from either TCL1 or TCL1/p66^{-/-} mice with overt leukemia. (Original magnification, 5x and 20x).

Figure S6. Flow cytometric analysis of intracellular Ki-67 in CD5⁺CD19⁺ leukemic cells of LN, liver and lung from either E μ -TCL1 (n=4) or E μ -TCL1/p66Shc^{-/-} (n \geq 4) mice with overt leukemia. Mean \pm SD. Error bars, SD. Mann Whitney Rank Sum test. p \leq 0.05, *.

Figure S7. Migration of splenic CD5⁺CD19⁺ cells from either wild-type (n=11) or p66Shc^{-/-} (n=11) mice and from E μ -TCL1 (n=15) or E μ -TCL1/p66Shc^{-/-} (n=15) mice with overt leukemia measured after a 3 h-treatment with 100 ng/ml CXCL12, MIP3- β , S1P, CCL2 or CXCL9. The data, obtained on duplicate samples from each mouse, are presented as

mean migration index (ratio migrated cells in chemokine-treated vs untreated samples) \pm SD. Anova one-way test, Multiple Comparison. $p \leq 0.001$, ***; $p \leq 0.01$, **; $p \leq 0.05$, *.

Figure S8. Quantitative RT-PCR analysis of CCR1 and CCR5 mRNA in leukemic cells from either wild-type (n=7) or p66Shc^{-/-} (n=8) mice and from E μ -TCL1 (n=12) or E μ -TCL1/p66Shc^{-/-} (n=13) mice with overt leukemia. The relative gene transcript abundance was determined on triplicate samples using the ddCt method. Mean \pm SD. Anova one-way test, Multiple Comparison. $p \leq 0.001$, ***; $p \leq 0.01$, **; $p \leq 0.05$, *.

Figure S9. A, B. Quantitative RT-PCR analysis of the p66Shc mRNA levels in B cells purified from CLL patients grouped as follows: **(A)** patients with wild-type chromosome 13 (chr 13 wt, n=22) or patients with 13q deletion (del 13q, n=55), according to chromosome 13 status; **(B)** patients with wild-type *TP53* (*TP53* wt, n=65) or patients with either mutated *TP53* or deleted chromosome 17 or both (*TP53* mut/del, n=7), according to the mutational status of *TP53* or of chromosome 17. The relative gene transcript abundance was determined on triplicate samples using the ddCt method. **C, D.** Quantitative RT-PCR analysis of the mRNA levels (left) and flow cytometric analysis of the surface levels (right) of CCR2 **(C)** and CXCR3 **(D)** in B cells purified from either healthy donors (HD) or CLL patients grouped in M-CLL and UM-CLL (qRT-PCR: HD, n=12; M-CLL, n=67; UM-CLL, n=64. Flow cytometric analysis: HD, n=7; M-CLL, n=11; UM-CLL, n=14). The relative gene transcript abundance was determined on triplicate samples using the ddCt method. Mean \pm SD. Anova one-way test, Multiple Comparison. $p \leq 0.001$, ***; $p \leq 0.01$, **; $p \leq 0.05$, *.

Figure S10. Correlation between the mRNA levels of p66Shc and the mRNA levels of CCR7 **(A)**, S1PR1 **(B)**, CXCR4 **(C)**, CCR2 **(D)** and CXCR3 **(E)** in B cells purified from CLL patients (n \leq 110). The relative gene transcript abundance was determined on triplicate

samples using the ddCt method. **F.** Quantitative RT-PCR analysis of the p66Shc mRNA levels in B cells purified from healthy donors (n=4) and in purified CLL B cells (n=6), nucleofected with either empty vector (CLL vect) or an expression construct encoding p66Shc (CLL p66). The relative gene transcript abundance was determined on triplicate samples using the ddCt method. Mean±SD. Anova one-way test, Multiple Comparison. $p \leq 0.0001$, ****; $p \leq 0.05$, *.

Figure S11. A. Quantitative RT-PCR analysis of p66Shc mRNA in B cells purified from CLL patients (n=157), grouped in “above threshold” (black box) and “below threshold” (0.24 threshold: mean ddct of p66Shc mRNA in all patients, grey box). The relative gene transcript abundance was determined on triplicate samples using the ddCt method. **B.** Immunoblot analysis with anti-Shc antibodies of postnuclear supernatants of B cells purified from healthy donors (Ctr) (n=3) or CLL patients, grouped in “above threshold” (n=4) and “below threshold” (n=4). The stripped filters were reprobated with anti-actin antibodies. Mean±SD. Mann Whitney Rank Sum test. $p \leq 0.001$, ***; $p \leq 0.01$, **.

Figure S12. A-D. EBV-B cells transfected with either scrambled siRNA or siRNA targeting *p66shc*. Assays were carried out 48 h after transfection (n=4). **A, B.** Immunoblot analysis with anti-Shc antibodies of postnuclear supernatants (**A**) and quantitative RT-PCR analysis of p66Shc mRNA (**B**) of EBV-B transfectants. The stripped filters were reprobated with anti-actin antibodies. The migration of molecular mass markers is indicated. **C.** Flow cytometric analysis of ROS production in the EBV-B transfectants loaded with the ROS-sensitive probe, CM-H₂DCFDA. Data refer to duplicate samples from 4 independent experiments. **D.** Flow cytometric analysis of the surface levels (left) and quantitative RT-PCR analysis of the mRNA levels (right) of CCR2 and CXCR3 in EBV-B transfectants. The relative gene

transcript abundance was determined on triplicate samples using the ddCt method.

Mean±SD. Mann Whitney Rank Sum test. $p \leq 0.001$, ***; $p \leq 0.01$, **.

Supplementary Tables.

Table S1. List of treatments and clinical parameters of 5 CLL patients grouped in “responding to” or “failing” Ibrutinib

	CLL patients responding to Ibrutinib		CLL patients failing Ibrutinib		
	# 1	# 2	# 3	# 4	# 5
1st therapy	FCR	FCR	FCR	BR	BR
IGHV status	Unmutated	Mutated	Mutated	Unmutated	Unmutated
TP53 status	Wild-type	Wild-type	Wild-type	Wild-type	Deleted
Response criteria iwCLL²	PR	PR	SD	SD	PD
Time to next treatment [months]	48	43	20	23	13
2nd line therapy	Ibrutinib	Ibrutinib	Ibrutinib	Ibrutinib	ibrutinib
TP53 status	Deleted and mutated	Mutated	Wild-type	Mutated	Deleted
Time point samples [months]	12	6	4	7	24
Last follow-up [months]	33	20	24	25	36
Response criteria iwCLL²	CR	PR	PD	PD	PD

FCR = fludarabine, cyclophosphamide and rituximab; BR = bendamustine and rituximab; iwCLL = international workshop on chronic lymphocytic leukemia; CR = complete response; PR = partial response; SD = stable disease; PD = progressive disease.

Table S2. List of the antibodies and reagents used in this study

Antibody/Reagent	Host	Clone	Source	Cat. N.	Concentration
Anti-CXCR4	Rabbit Mouse	- 12G5	AbCam R&D	AB124824 FAB170P	1:200 1:50
Anti-CCR7	Rabbit Mouse	Y59 150503	Novus Biologicals R&D	NB110-55680 FAB197F	1:500 1:50
Anti-CCR2	Rabbit	-	Invitrogen	PA5-23043	1:50
Anti-CXCR3	Rabbit	-	Invitrogen	71-8800	1:50
Anti-S1PR1	Rabbit	-	Novus Biologicals	NB110-93513	1:100
Anti-CD45R	Rat	9F14	Genetex Int.	GTX53152	1:150
Anti-Bcl-2	Mouse	C2	Santa-Cruz	sc-7382	1:500
Anti-Bax	Mouse	6A7	BD Pharmingen	556467	1:500
Anti-Shc	Rabbit	-	EMD Millipore	06-203	1:500
Anti-STAT4	Rabbit	-	Cell Signaling	2653S	1:500
Ki-67	Rabbit	-	AbCam	AB15580	1:200
Anti-actin	Mouse	C4	Merk Millipore	MAB1501	1:2000
Fc-Block	Rat	2.4G2	BD Biosciences	553141	1:50
FITC anti-mouse CD19	Rat	1D3	BD pharmingen	553785	1:40
PE anti-mouse CD5	Rat	53 - 7.3	BD pharmingen	553022	1:40
Per-CP anti-mouse IgM	Rat	RMM-1	BioLegend	406512	1:30
Alexa Fluor anti-Rabbit 488	Goat	-	Invitrogen	A11008	1:400

Anti-Rat IgG	Rabbit	-	AbCam	AB6734	1:400
CXCL12	-	-	Sigma-Aldrich	SRP4388	100 ng/ml
MIP-3β	-	-	Sigma-Aldrich	SRP4495	100 ng/ml
CCL2	-	-	R&D systems	479-JE	100 ng/ml
CXCL9	-	-	R&D systems	492-MM	100 ng/ml
S1P	-	-	Sigma-Aldrich	73914	100 nM
Fludarabine phosphate	-	-	Sigma-Aldrich	F9813	35 μ M
Ibrutinib	-	-	SelleckChem	S2680	1 μ M
H₂O₂	-	-	Sigma-Aldrich	95299	50 μ M
CM-H₂DCFDA	-	-	Invitrogen	C6827	5 μ M
p66Shc-1 siRNA	-	-	GenScript Corporation	-	10 pg/10 ⁶ cells
RLUC esiRNA	-	-	Sigma-Aldrich	EHURLUC	10 pg/10 ⁶ cells

Table S3. List of the primers used in this study

Quantitative RT-PCR	Forward 5'-3'	Reverse 5'-3'
Human p66Shc	TCC GGA ATG AGT CTC TGT CA	GAA GGA GCA CAG GGT AGT GG
Mouse p66Shc	TGA GTT GGG AGA GCA GAG GT	CTC ATT CCG AAG TGG GTT GT
Mouse Bax	TGC AGA GGA TGA TTG CTG AC	GAT CAG CTC GGG CAC TTT AG
Mouse Bcl-2	GGA CTT GAA GTG CCA TTG GT	AGC CCC TC GTG ACA GCT TA
Mouse Mcl-1	GAA GGC GGC ATC AGA AAT GT	GCA GCT TCA AGT CCA CCT TC
Mouse CXCR4	TCC TCC TGA CTA TAC CTG ACT TC	GAC GAG ACC CAC CAT TAT ATG C
Mouse CCR7	GTG AGC ATG GAG GCG GAG AC	CAG CAG CAA TTC GGT GGA TGG
Mouse S1PR1	TTC CGC AAG AAC ATC TCC AAG	CAG CCC ACA TCT AAC AGT AGT
Mouse CCR2	TGA GAA GAA GAG GCA CAG GG	ATG GCC TGG TCT AAG TGC TT
Mouse CXCR3	GGG GTC TCT GTC TGC TCT TT	CCT CAT AGC TCG AAA ACG CC
Mouse CCR1	CCA TGC CAA AAG ACT GCT GT	AGA GAC AGC CAG GTT GAA CA
Mouse CCR5	ATT CTC CAC ACC CTG TTT CG	CAG GGT TTA GGC AGC AGT GT
Mouse CXCR5	TCC TAC TAC CGA TGC TTG TGA	CCG CCT TCT GCC GCT GAG
Mouse GAPDH	AAC GAC CCC TTC ATT GAC	TCC ACG ACA TAC TCA GCA C

Screening PCR	Forward 5'-3'	Reverse 5'-3'
TCL1	GAC ACT CGG GGA GGC AGT CA	GTG AAT TCT TTG CCA AAG TGA
p66Shc 550 bp	CCT CCC CAG GTC ATC TGT TAT CAT	CTC GTG TGG GCT TAT TGA CAA AG
p66Shc 300 bp	GGG TGG AGA GGC TTT TTG CTT C	CTC GTG TGG GCT TAT TGA CAA AG
<i>Trp53</i> amplification	Forward 5'-3'	Reverse 5'-3'
Fragment I (nt -143→+356)	TGC TCA CCC TGG CTA AAG TT	GGA GGA GAG TAC GTG CAC AT
Fragment II (nt +242→+776)	GCC CCT GTC ATC TTT TGT CC	CTG TCC CGT CCC AGA AGG
Fragment III (nt +711→+1265)	CGC CGA CCT ATC CTT ACC AT	TAA GAC AGC AAG GAG AGG GG

Table S4. Length and weight of spleens from C57BL/6, C57/p66^{-/-}, Eμ-TCL1 and Eμ-TCL1/p66^{-/-} mice.

	C57BL/6 (n=6)	C57/p66^{-/-} (n=5)	Eμ-TCL1(n=10)	Eμ-TCL1/p66^{-/-} (n=16)
Spleen length (cm)	1.38 ± 0.13	1.44 ± 0.11	2.44 ± 0.59 <i>**p≤0.01 vs C57BL/6</i>	2.38 ± 0.73 <i>**p≤0.01 vs C57BL/6</i>
Spleen weight (gr)	0.12 ± 0.05	0.12 ± 0.02	1.61 ± 0.66 <i>***p≤0.001 vs C57BL/6</i>	1.66 ± 1.05 <i>***p≤0.001 vs C57BL/6</i>